NJC

PAPER

View Article Online
View Journal

Cite this: DOI: 10.1039/c9nj01114e

New molecular design for blue BODIPYs†

Zhiyuan Wu, [a] Hikaru Fujita, [a] Nikki Cecil M. Magdaong, [b] James R. Diers, [c] Don Hood, [b] Srinivasarao Allu, [a] Dariusz M. Niedzwiedzki, [d] Christine Kirmaier, [b] David F. Bocian, *[c] Dewey Holten *[b] and Jonathan S. Lindsey *[a]

Received 2nd March 2019,
Accepted 7th April 2019

DOI: 10.1039/c9nj01114e

rsc.li/njc

Diverse dihydrodipyrrins are available as precursors in the *de novo* synthesis of bacteriochlorins and chlorins. Each dihydrodipyrrin contains one pyrrole and one pyrroline (3,4-dihydropyrrole) ring joined at the respective α-positions *via* a methylene unit as well as a geminal-dimethyl group at one of the pyrroline β-positions. Complexation of the dihydrodipyrrin ligands occurs smoothly upon treatment with Bu_2B–OTf or $BF_3{\cdot}OEt_2$ in dichloromethane containing triethylamine at room temperature. Six such dihydrodipyrrinatoboron complexes have been prepared and are examined here. The complexes with $-BF_2$ or $-BBu_2$ absorb in the blue region ($\lambda_{abs} \sim 400$ nm) and fluoresce ($\lambda_{em} \sim 500$ nm) with large Stokes shift (~100–150 nm), almost no absorption-fluorescence spectral overlap, and high fluorescence quantum yield ($\Phi_f \sim 0.4$–0.9). The spectral features are rather insensitive to substituents in the pyrrole nucleus (carboethoxy, bromo, and *p*-tolyl) and the presence of a 1-naphthalenyl group at the *meso*-position. In one case examined, the spectral properties including Φ_f value were almost identical in toluene and acetonitrile. The blue BODIPYs may be useful as broadband photosensitizers upon violet-laser excitation.

Introduction

The discovery of dipyrrinatoboron difluoride complexes half a century ago ushered in a rich new era of research.[1] BODIPYs afford many attractive features: (1) strong absorption and fluorescence ($\varepsilon \sim 5 \times 10^4$ M^{-1} cm^{-1}; Φ_f up to nearly unity) in the visible region; (2) neutral chromophore rather than charged as is the case with many dyes, thereby facilitating handing; (3) facile synthetic access from the corresponding dipyrrin or dipyrromethane (upon oxidation and complexation in a one-flask process); and (4) malleable molecular design with regards to bathochromic tuning of the key spectral features.[2–11] Interest shows no sign of abating; >4600 papers in the past decade are elicited upon searching "BODIPY" in Web of Science, more than 5 times that in the preceding decade.

The parent BODIPY (**I**, Chart 1) absorbs and fluoresces near 500 nm. While addition of conjugated groups has given rise to BODIPYs with spectral features shifted to the red and even near-infrared region,[3,8,11] designs for hypsochromic shifting have been less forthcoming. The chief molecular design for hypsochromic shifting entails installation of an amino group at the *meso*-position of the dipyrrin ligand. With the amino group alone (**II**), the absorption shifts to ~400 nm and a high Φ_f value is retained. But a mere change to an alkylamino group (**III**) causes significant diminution of the fluorescence yield. A further limitation of the *meso*-amino strategy, at least in some cases, is that the *meso*-position is attractive for installation of synthetic handles (*via* the corresponding and readily accessible *meso*-substituted dipyrromethanes). Here, we describe a new molecular design for BODIPYs that absorb in the blue spectral region. The design was arrived at

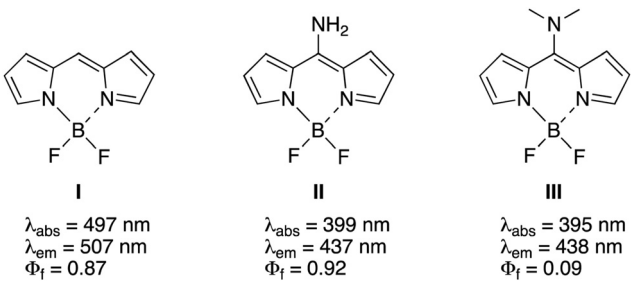

Chart 1 Parent BODIPY and prior "blue" analogues.

[a] Department of Chemistry, North Carolina State University, Raleigh, North Carolina 27695-8204, USA. E-mail: jlindsey@ncsu.edu; Tel: +1-919-515-6406
[b] Department of Chemistry, Washington University, St. Louis, Missouri 63130-4889, USA. E-mail: holten@wustl.edu; Tel: +1-314-935-6502
[c] Department of Chemistry, University of California, Riverside, California 92521-0403, USA. E-mail: david.bocian@ucr.edu; Tel: +1-951-827-3660
[d] Department of Energy, Environmental & Chemical Engineering, and Center for Solar Energy and Energy Storage, Washington University, St. Louis, Missouri 63130-4889, USA

† Electronic supplementary information (ESI) available: Photophysical data; characterization data including NMR spectra for all new compounds; and single-crystal X-ray data. CCDC 1900105 (**1-BBu$_2$**), 1900106 (**2-BBu$_2$**) and 1900107 (**2-BF$_2$**). For ESI and crystallographic data in CIF or other electronic format see DOI: 10.1039/c9nj01114e

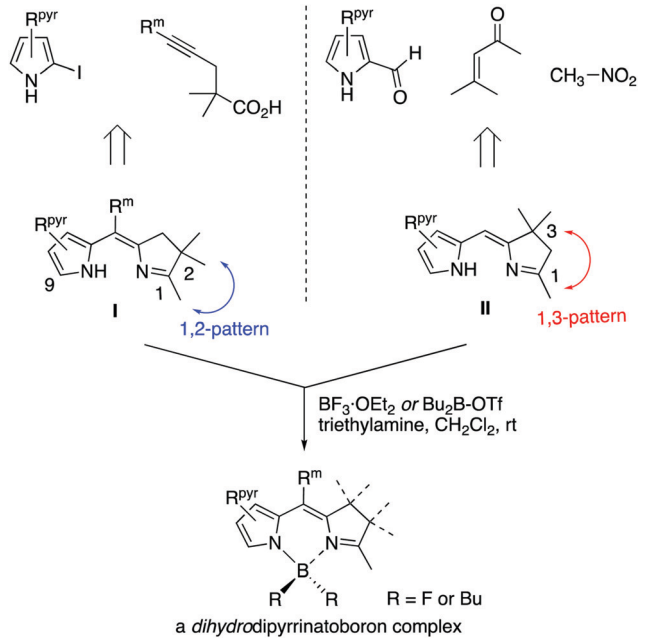

Scheme 1 Retrosynthesis of dihydrodipyrrin ligands and boron complexes.

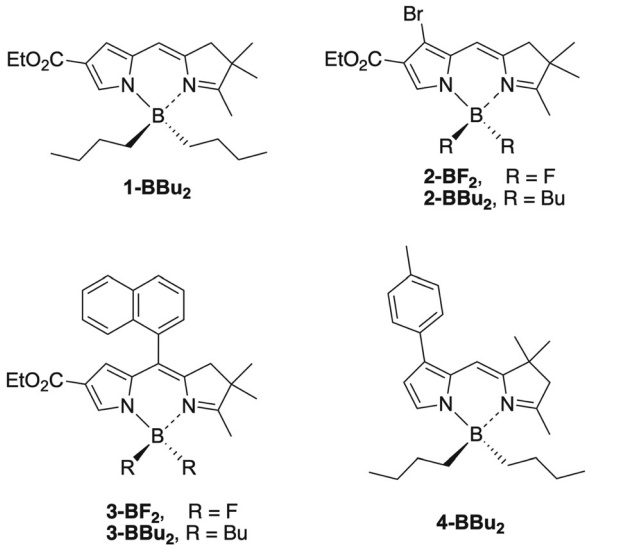

Chart 2 Dihydrodipyrrinatoboron complexes.

serendipitously during the course of fundamental studies concerning bacteriochlorin synthesis methodology.

The *de novo* synthesis of bacteriochlorins relies on the self-condensation of dihydrodipyrrin species.[12,13] Two complementary routes (Scheme 1) readily afford diverse dihydrodipyrrins that vary in substituents at the pyrrolic positions (R^{pyr}), the *meso*-position (R^{m}), and the location of the *gem*-dimethyl group in the pyrroline ring. The *gem*-dimethyl group is essential to block inadvertent oxidation leading to the corresponding dipyrrin. We earlier had employed complexation with dialkylboron reagents to facilitate purification of acyldipyrromethanes[14,15] and alter substitution reactions of tetrahydrodipyrrins.[16] Here we report analogous studies with a collection of dihydrodipyrrins and characterize the resulting absorption and fluorescence features of the dihydrodipyrrinatoboron species. The spectroscopic features including broad absorption at ~400 nm and broad yet strong fluorescence centered at ~500 nm are more reminiscent of aminocoumarins[17] than the parent dipyrrinatoboron complexes. Such features may support broad-band photosensitization upon violet-laser excitation (405 nm) and microscopy applications where a large Stokes shift is desirable.

Results and discussion

Synthesis

We prepared a handful of boron complexes from available dihydrodipyrrin ligands **1**,[12] **2**,[18] **3**,[18] and **4**[16] (Chart 2). Each dihydrodipyrrin contains a *gem*-dimethyl group in the 2- or 3-position depending on the synthetic method of preparation, a 1-methyl group, and one or two (carboethoxy, bromo, 1-naphthenyl, *p*-tolyl) substituents that together enable an initial assessment of substituent effects on spectroscopic features.

Dihydrodipyrrin **1** is known[12] but was prepared here in a streamlined manner, which illustrates the simplicity of the synthesis. The Pd-mediated coupling of 2-iodopyrrole **5**[12] and pentynoic acid **6**[12] afforded the pyrrole–lactone **7** (80% yield *versus* 55% previously), which upon reaction with the Petasis reagent gave pyrrole–ene–lactone **8** (Scheme 2). Reaction of **8** *via* a process similar to a Paal–Knorr reaction gave dihydrodipyrrin **1** along with putative isomer **1*E***. Such isomers have been inferred previously[19] on the basis of ^{1}H NMR spectroscopy. Treatment of the crude mixture containing **1** and **1*E*** with triethylamine and dibutylboron triflate gave the desired complex in 52% yield (from **8**). Crystals of **1-BBu$_2$** suitable for X-ray analysis were obtained by slow evaporation of a solution of hexanes/chloroform at room temperature.

As shown for the preparation of **1-BBu$_2$**, the complexation procedure is simple – treatment of the dihydrodipyrrin ligand with Bu_2B–OTf[16] or $BF_3{\cdot}OEt_2$[2] in dichloromethane containing triethylamine at room temperature readily affords the corresponding $-BF_2$ or $-BBu_2$ complex, respectively. In this manner, complexes **2-BBu$_2$** (1 h, 85% yield), **2-BF$_2$** (2 h, 93%), **3-BF$_2$** (overnight, 86%), and **3-BBu$_2$** (overnight, 71%) were obtained as yellowish solids with bright yellow-green fluorescence in solution. Complex **4-BBu$_2$** was prepared previously.[16] The complexes are stable under routine handling to air and moisture, and were readily purified by chromatography and/or crystallization, although **2-BF$_2$** slowly decomposed upon TLC analysis (silica or Si-diol) at room temperature. On the limited comparison of two pairs of compounds, the $-BBu_2$ complexes were more stable than the $-BF_2$ complexes. Crystals of **2-BBu$_2$** and **2-BF$_2$** suitable for X-ray analysis were obtained from vapor diffusion of hexanes to ethyl acetate solution at room temperature. While attempts at synthetic manipulations of the dihydrodipyrrin–boron complexes were very limited, attempts to debrominate **2-BBu$_2$** to give **1-BBu$_2$** with *n*-butyllithium or the isopropylmagnesium chloride lithium chloride complex were unsuccessful.

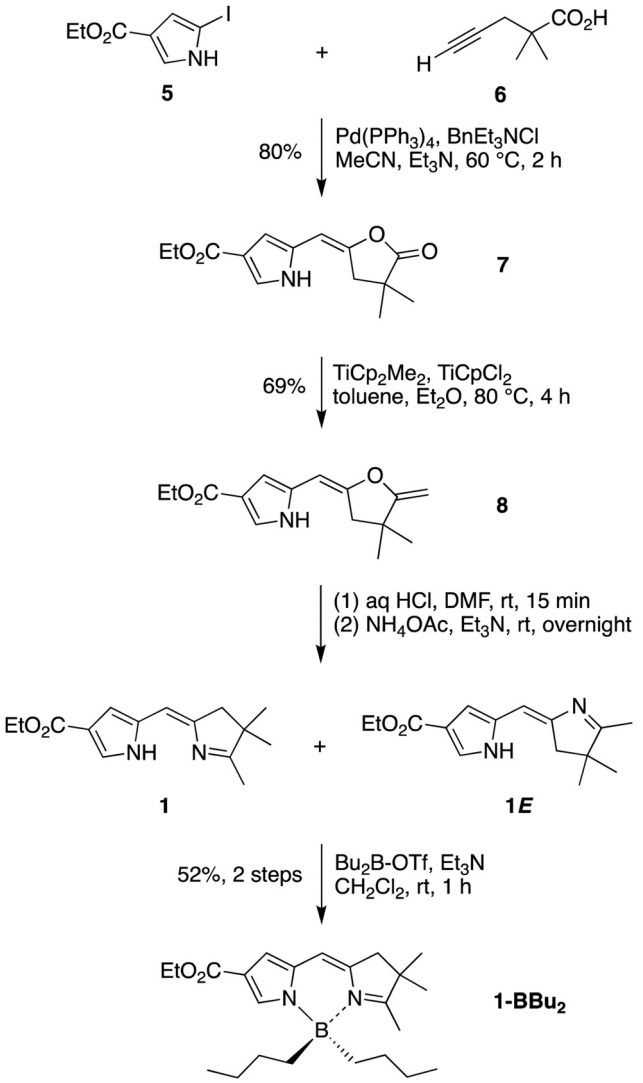

Scheme 2 The synthesis of dihydrodipyrrin complex **1-BBu$_2$**.

Chemical characterization

Each boron complex was examined by ^{11}B NMR spectroscopy using B(OH)$_3$ (19.8 ppm in DMF[20]) as a standard. Each boron complex exhibited a broad peak in the range 0.95–3.70 ppm, to be compared with that of similar compounds such as *N*-(9-borabicyclo[3.3.1]non-9-yl)pyrrole (59.9 ppm)[21] and the 9-BBN complex of 1-acyldipyrromethanes (~13 ppm).[14] The relative upfield shift of the complex is characteristic for species wherein boron is coordinated with an N_{imino} nitrogen.[22]

X-ray structural analysis was performed on the **1-BBu$_2$**, **2-BBu$_2$**, and **2-BF$_2$** complexes. The ORTEP diagrams are shown in Fig. 1, and the crystallographic data are listed in Table S1 (ESI†). For **1-BBu$_2$**, with the lack of a bromine substituent, there is a significant amount of positional disorder in the ring system and the *n*-butyl groups. The crystal was well formed, but shattered when placed in a cold stream of nitrogen on the instrument. The data collection was performed at a higher temperature (180 K) than typical (100 K). The overall effect is that the resolution and high-angle intensity of the data are only suitable for establishing connectivity within the molecule.

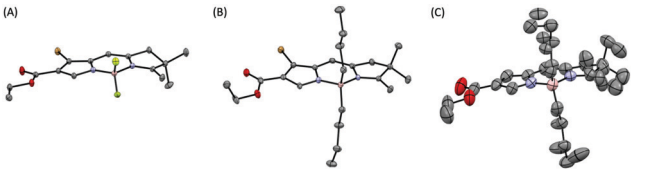

Fig. 1 ORTEP diagrams (contoured at the 50% level with omission of H atoms) for the single-crystal X-ray data of (A) **2-BF$_2$**, (B) **2-BBu$_2$**, and (C) **1-BBu$_2$**. The larger display for **1-BBu$_2$** reflects disorder, which may in part reflect the temperature of collection (180 K) *versus* that of **2-BF$_2$** and **2-BBu$_2$** (100 K). Atom coloration: N, blue; O, red; B, pink; F, lime green.

Spectroscopic features

The complexes were characterized by static and time-resolved absorption and fluorescence spectroscopy. Fig. 2 shows the static absorption and fluorescence emission spectra of the boron–dihydrodipyrrins in toluene. Fig. 3 shows the spectra for a representative compound, **1-BBu$_2$** in toluene, acetonitrile and dimethylsulfoxide. The peak wavelengths are listed in Table 1. The molar absorption coefficients of all six dihydrodipyrrinato-boron complexes were measured (Table S2, ESI†). In general, the long-wavelength absorption band exhibits a molar absorption coefficient value of $\sim 10^4$ M^{-1} cm^{-1} in toluene at room temperature. Several compounds also were examined in acetonitrile, where values quite similar to those in toluene also were obtained.

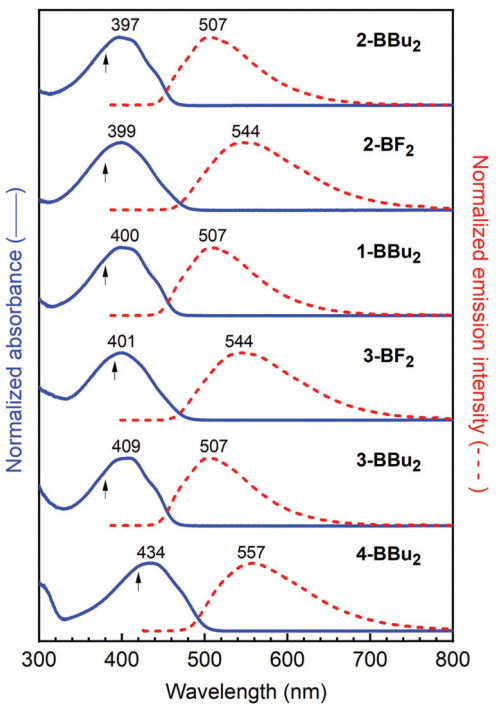

Fig. 2 Absorption spectra (blue solid) and fluorescence emission spectra (red dashed) of boron–dihydrodipyrrins in toluene. Arrows indicate the excitation wavelength used to obtain each emission spectrum. The same emission spectra were obtained using other excitation wavelengths.

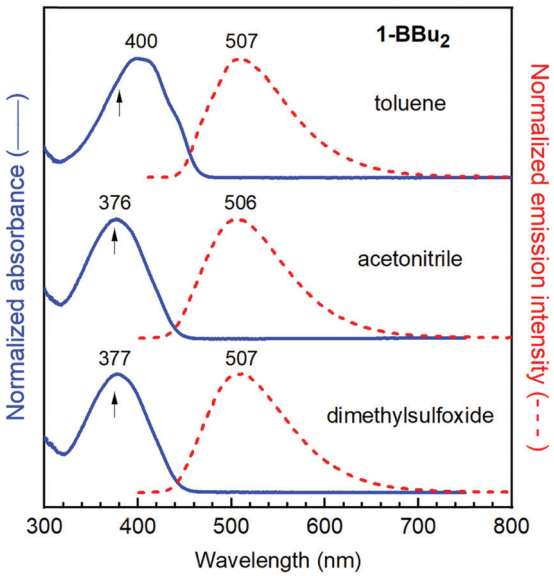

Fig. 3 Absorption spectra (blue solid) and fluorescence emission spectra (red dashed) of boron–dihydrodipyrrin **1-BBu$_2$** in toluene, acetonitrile and dimethylsulfoxide. Arrows indicate the excitation wavelength used to obtain each emission spectrum. The same emission spectra were obtained using other excitation wavelengths.

Comparing pairs **2-BF$_2$** *versus* **2-BBu$_2$** and **3-BF$_2$** *versus* **3-BBu$_2$**, the absorption maximum of the difluoro construct differs by ≤8 nm compared to the dibutyl analogue. More dramatically, the fluorescence peak is bathochromically shifted by 37 nm in the fluoro- *versus* butyl-containing compounds. Thus, the Stokes shift between the fluorescence and absorption maxima of 98–110 nm for the dibutyl-bearing constructs is increased to 143–145 nm for the difluoro analogues (Fig. 2 and Table 1). Increasing the solvent dielectric constant [toluene (2.38) < acetonitrile (37.5) < dimethylsulfoxide (46.7)] for **1-BBu$_2$** results in a substantial hypsochromic shift of the absorption maximum (400 nm < 376 nm ~ 377 nm) without much change in the fluorescence peak position (507 nm ~ 506 nm ~ 507 nm). Thus, the Stokes shift for **1-BBu$_2$** increases from 107 nm in toluene to 130 nm in acetonitrile and dimethylsulfoxide (Fig. 3 and Table 1).

Fluorescence yields were determined with respect to two standards using several excitation wavelengths, with good agreement among the results for each compound. The results of the individual measurements are given in Table S3 (ESI†) and the average values in Table 1. The Φ_f values range from 0.87 for the simplest of the compounds (**1-BBu$_2$**) to 0.30 for the analogue that bears 7-*p*-tolyl and 3-*gem*-dimethyl substituents (**4-BBu$_2$**). The emission yield is also quite high for **3-BBu$_2$** (0.88) and **2-BBu$_2$** (0.81), but is roughly half as large for counterparts **3-BF$_2$** (0.38) and **2-BF$_2$** (0.42). Our prior studies on boron–dipyrrins (not boron–dihydrodipyrrins) bearing a 5-mesityl group and no other substituents show that two fluorines on boron affords a greater Φ_f (0.93) than two methyl groups (0.33).[24] The interplay between substituents on the boron and dihydrodipyrrin (or dipyrrin) framework on the excited-state decays will be discussed further below.

The excited-state decay routes and dynamics were investigated by transient absorption (TA) and time-resolved fluorescence spectroscopies. The S_1 lifetimes determined by the various methods are listed in Table S3 (ESI†) and the average values in Table 1. Representative TA difference spectra for **3-BBu$_2$** are shown in Fig. 4A. The negative-going features in the TA difference spectra (excited minus ground state) are bleaching of the $S_0 \rightarrow S_1$ absorption at ~400 nm and $S_1 \rightarrow S_0$ stimulated emission at ~540 nm, positions that are consistent with features in the static absorption and fluorescence spectra (Fig. 4B). The TA difference spectra also show a prominent excited-state absorption (*e.g.* $S_1 \rightarrow S_3$) at ~460 nm that has an extinction coefficient substantially greater than that for the $S_0 \rightarrow S_1$ transition in the ground-state absorption spectrum. The spectral evolution displayed in Fig. 4A and the representative kinetic traces in Fig. 4C show only minor changes over the first few hundred picoseconds with time constants of ~5 and ~60 ps that likely represent some combination of vibrational, solvent or conformational relaxations in the S_1 excited state accompanied by little ground-state recovery. The S_1 excited-state decay occurs for **3-BBu$_2$** in toluene with a time constant of 7 ns. The TA data show that during this time S_1 decays essentially completely to the ground state, with virtually no formation of the lowest triplet excited state by $S_1 \rightarrow T_1$ intersystem crossing. Thus, for all practical purposes the yields of $S_1 \rightarrow S_0$ fluorescence and

Table 1 Photophysical properties[a]

Compound	Solvent	λ_{abs}[b] calc. (nm)	λ_{abs} (nm)	λ_{em} (nm)	Stokes shift (nm)	Stokes shift (cm^{-1})	Φ_f[c]	τ_s[d] (ns)	k_f^{-1}[e] (ns)	k_{ic}^{-1}[e] (ns)
1-BBu$_2$	Toluene	399	400	507	107	528	0.87 ± 0.04	7.5 ± 0.8	8.7	56
1-BBu$_2$	MeCN	373	376	506	130	683	0.88 ± 0.04	8.8 ± 0.3	10	75
1-BBu$_2$	DMSO	373	377	507	130	680	0.90 ± 0.04	7.9 ± 0.2	8.7	77
2-BBu$_2$	Toluene	397	397	507	110	547	0.81 ± 0.01	7.0 ± 0.5	8.6	37
2-BF$_2$	Toluene	399	399	544	145	668	0.42 ± 0.01	4.9 ± 0.2	12	8.4
3-BBu$_2$	Toluene	400	409	507	98	473	0.88 ± 0.03	7.0 ± 0.7	8.0	59
3-BF$_2$	Toluene	404	401	544	143	656	0.38 ± 0.04	4.9 ± 0.1	13	7.8
4-BBu$_2$	Toluene	431	434	557	123	509	0.30 ± 0.04	3.9 ± 0.1	13	5.5

[a] All data were acquired at room temperature. MeCN is acetonitrile and DMSO is dimethylsulfoxide. [b] The $S_0 \rightarrow S_1$ transition wavelength calculated by TDDFT was shifted to lower energy in all cases by 2500 cm^{-1} to obtain better overall agreement with the measured spectra. [c] Fluorescence yields were determined for deoxygenated samples relative to the standards pyranine (Φ_f = 1.0 in 0.10 M NaOH[23]) and 5-mesityldipyrrinatoboron difluoride (Φ_f = 0.93 in toluene[24]) and averaged (Table S3, ESI). [d] Singlet excited-state lifetimes are the average of results from three methods; see Table S3 (ESI). [e] S_1 decay rate constants were derived as described in the text.

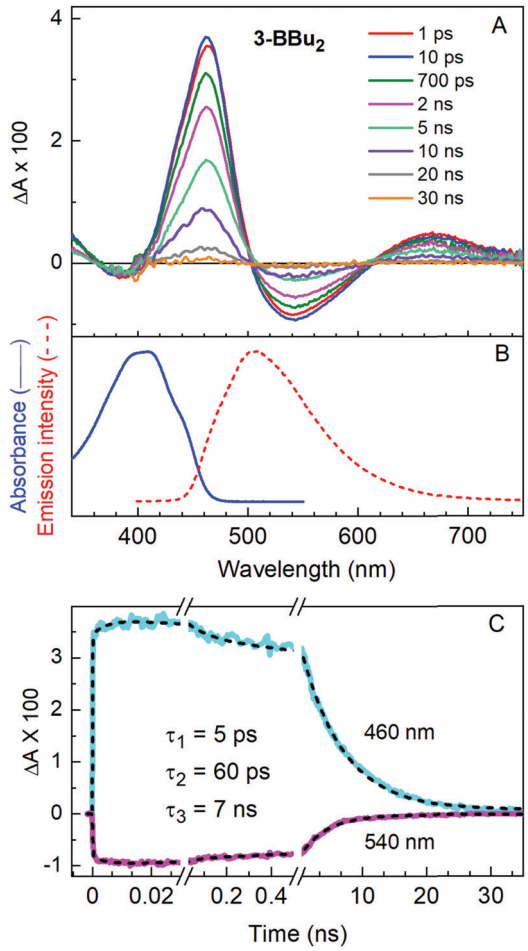

Fig. 4 TA difference spectra (A), static absorption (blue solid) and fluorescence (red dashed) spectra (B), and kinetic trace (C) of **3-BBu$_2$** in toluene. The TA studies used 100 fs excitation flashes at 400 nm.

$S_1 \rightarrow S_0$ internal conversion sum to unity ($\Phi_f + \Phi_{ic} \sim 1$). The corresponding rate constants can be calculated from the expressions $k_f = \Phi_f/\tau_S$ and $k_{ic} = (1 - \Phi_f)/\tau_S$. The values for **3-BBu$_2$** in toluene are given in Table 1.

Similar TA and fluorescence decay results were obtained for **3-BBu$_2$** in acetonitrile and dimethylsulfoxide. The analogous measurements for all the other boron–dihydrodipyrrins in toluene also showed no significant triplet yield, and S_1 lifetimes roughly in the 4–7 ns range (Table 1). The low T_1 yields indicate that the rate constant for intersystem crossing is very small relative to those for fluorescence and internal conversion (Table 1), likely $<(1\ \mu s)^{-1}$. Thus, even if the bromine substituent in **1-BBu$_2$** and **3-BBu$_2$** gives a heavy-atom enhancement of the $S_1 \rightarrow T_1$ rate constant, the magnitude is still apparently not great enough to give a measurable triplet yield and commensurate reduction in Φ_f and τ_S compared to analogues that lack the halogen atom.

Examination of Table 1 shows that the derived rate constant for $S_1 \rightarrow S_0$ fluorescence (k_f) varies little among the compounds. This is consistent with the comparable extinction coefficients for $S_0 \rightarrow S_1$ absorption (Table S2, ESI†), the two quantities being connected by the relationships between the Einstein coefficients.[25] The derived rate constants for $S_1 \rightarrow S_0$ internal conversion (k_{ic}) for **2-BF$_2$** and **3-BF$_2$** are 4–8 fold greater than those for **1-BBu$_2$**, **2-BBu$_2$**, and **3-BBu$_2$** but comparable to that for **4-BBu$_2$**. Prior work[24,26] on boron–dipyrrins (not dihydrodipyrrins) that vary in the presence and type of aryl ring at the 5 (*meso*) position, two fluorines or two alkyl groups on boron, along with the presence, number and types of alkyl groups at the 2, 3, 7, and 8 positions suggests that the combination of substituents can impact the rate constant and yield for non-radiative deactivation *via* internal conversion by allowing or suppressing motions that alter the planarity of the dipyrrin framework and the rotation of the aryl ring. It is reasonable that such motions are influenced by interplay of the substituents on the dihydrodipyrrin and boron (Chart 2) and impact internal conversion and thus Φ_f and τ_S for the compounds studied herein.

Calculations using density functional theory (DFT) and the time-dependent extension TDDFT were undertaken to gain further insights into the relationships between chemical composition, electronic structure and photophysical properties of the boron–dihydrodipyrrins. The electron-density distribution of the highest occupied molecular orbital (HOMO) and of the lowest unoccupied molecular orbital (LUMO) for each compound are shown in Fig. 5. Below each orbital is the calculated energy in toluene (upper value) and in acetonitrile (lower value). Below the structure of each compound is the corresponding $S_0 \rightarrow S_1$ transition energy, wavelength and oscillator strength calculated by TDDFT in the two solvents. The calculated transition wavelengths generally reproduce several key trends (Fig. 5 and Table 1), which include (1) the bathochromic shift of **4-BBu$_2$** relative to the other analogues, and (2) the hypsochromic shift for **2-BBu$_2$** in polar *versus* nonpolar media.

The MOs for **2-BBu$_2$** also show that there is considerable electron density on the bromine and adjacent positions on the dihydrodipyrrin. Thus, the lack of an effect of the bromine on the Φ_f and τ_S values of **2-BBu$_2$** relative to the other dihydrodipyrrin complexes studied cannot be attributed to a lack of communication between the halogen and the π-system of the dihydrodipyrrin. This finding tends to reinforce the view noted above that these molecules appear to have very small spin–orbit coupling and thus small rate constants for $S_1 \rightarrow T_1$ intersystem crossing. Accordingly, any heavy-atom enhancement does not increase k_{isc} sufficiently to give effective competition with k_f and k_{ic}, which dominate the excited-state dynamics of the boron–dihydrodipyrrins.

The spectral properties of the blue BODIPYs described herein can be compared with other blue-absorbing fluorophores. The absorption and fluorescence spectra of **1-BBu$_2$**, the 5-amino-dipyrrinatoboron difluoride **II**, and coumarin 151 are shown in Fig. 6 and summarized in Table 2. Compared with **II**, **1-BBu$_2$** absorbs at nearly the same wavelength but with a substantially broader absorption band (85 *versus* 48 nm), larger Stokes shift (107 *versus* 39 nm), and comparable (and strong) Φ_f value. Compared with coumarin 151,[27,28] **1-BBu$_2$** exhibits similar absorption features and Stokes shift although **1-BBu$_2$** exhibits a broader emission band and larger Φ_f value. In this regard, the Φ_f value of coumarin 151 increases substantially with increasing solvent polarity (*e.g.*, 0.17 in 3-methylpentane; 0.57 in acetonitrile)[27] whereas that of **1-BBu$_2$** is 0.87–0.90 in solvents having a wide range of polarity (toluene, acetonitrile and dimethylsulfoxide).

Name	Structure ($S_0 \rightarrow S_1$: λ, f)	HOMO (energy, eV)	LUMO (energy, eV)
1-BBu$_2$	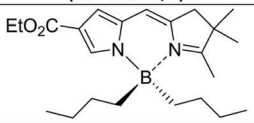	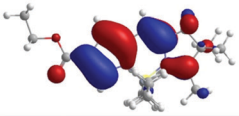	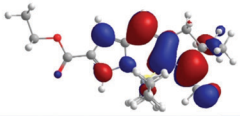
	399 nm, 0.52 373 nm, 0.52	−7.11 −7.26	−0.18 −0.09
2-BBu$_2$	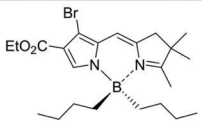	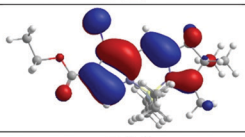	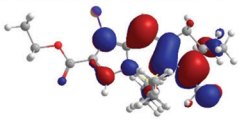
	397 nm, 0.57 372 nm, 0.57	−7.26 −7.39	−0.31 −0.22
2-BF$_2$	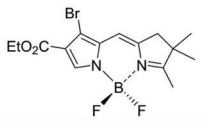	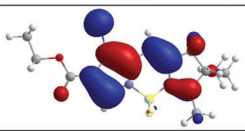	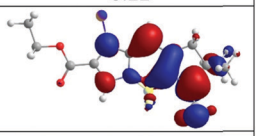
	399 nm, 0.61 373 nm, 0.60	−7.49 −7.64	−0.59 −0.51
3-BBu$_2$	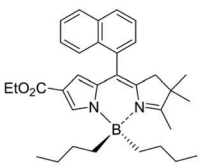	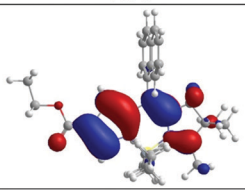	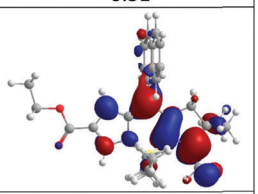
	400 nm, 0.49 373 nm, 0.48	−7.11 −7.29	−0.20 −0.13
3-BF$_2$	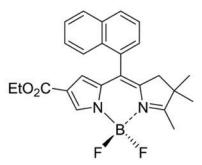	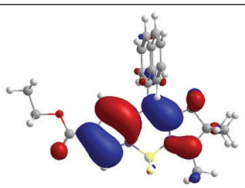	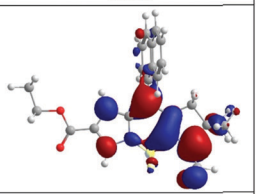
	404 nm, 0.51 376 nm. 0.50	−7.36 −7.55	−0.48 −0.45
4-BBu$_2$	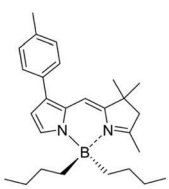	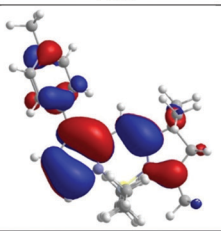	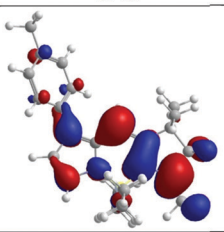
	431 nm, 0.53 403 nm, 0.54	−6.72 −6.88	−0.08 −0.03

Fig. 5 Results of DFT and TDDFT calculations for the boron–dihydrodipyrrins. Below each MO, the upper value is the calculated energy in toluene and the lower value is for acetonitrile. Below each structure are the calculated $S_0 \rightarrow S_1$ absorption wavelength (*λ*) and oscillator strength (*f*), with the top values being for toluene and the lower ones for acetonitrile. The transition energies are all arbitrarily shifted to lower energy by 2500 cm^{-1} to give better agreement with the measured spectra (Table 1); this systematic shift does not affect the calculated trends with compound or medium.

We also note that the molar absorption coefficient of **II** in methanol was reported as 2.6×10^4 M^{-1} cm^{-1} in 2011[29] (see Fig. 6 and Table 2) and as 1.12×10^5 M^{-1} cm^{-1} in 2013.[30]

Outlook

The results reported herein indicate a new molecular design for achieving blue absorption in the general BODIPY family. The following points appear noteworthy. First, the sizable Stokes shift with almost no overlap[32] of the absorption and fluorescence bands suggests applications for broad-band photosensitization upon violet-laser (405 nm) excitation or use in stimulated emission depletion (STED) microscopy[33] where the large Stokes shift is essential. Second, the spectral features resemble those of members of the aminocoumarin family,[17,27,28,31] although more extensive

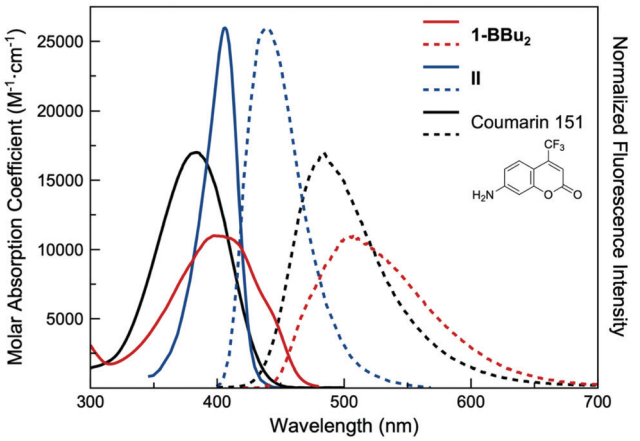

Fig. 6 Absorption and fluorescence emission spectra of **1-BBu$_2$**, **II**, and coumarin 151. The absorption spectra are shown (solid lines) according to their molar absorption coefficient. For each compound, the emission intensity is adjusted commensurably (dashed lines).

Table 2 Photophysical properties of **1-BBu$_2$**, **II** and coumarin 151

Compound	λ_{abs} (nm)	ε_{abs} (M^{-1} cm^{-1})	fwhm (nm)	λ_{em} (nm)	Stokes (nm)	Φ_f
1-BBu$_2$[a]	400	1.1×10^4	85	507	107	0.87
II[b]	399	2.6×10^4	48	438	39	0.92
Coumarin 151[c]	384	1.7×10^4	67	484	100	0.53

[a] In toluene. [b] In methanol.[29] [c] In ethanol.[31]

studies (*e.g.*, photostability) are required for in-depth comparisons. Third, use of the dihydrodipyrrin (*versus* the 5-aminodipyrrin) to achieve short-wavelength absorption leaves open the 5-position for synthetic manipulation, such as for incorporation into arrays or attachment of bioconjugation handles. Fourth, the dihydrodipyrrinatoboron complexes are neutral fluorophores,[2] like BODIPYS, and hence can be tailored for use in diverse (organic or aqueous) media. Fifth, owing to two complementary routes to dihydrodipyrrins (Scheme 1), synthetic capabilities are available for facile molecular tailoring of the three pyrrole positions, the *gem*-disubstitution site (enabling swallowtail architectures[34]), the 5-position, and the pyrroline 1-position. Finally, numerous dihydrodipyrrins are known,[12,13] indicating the untapped potential for development of an in-depth structure–activity relationship concerning tailored blue-absorbing/emitting complexes.

Experimental section

General methods

^{1}H and ^{13}C NMR spectra were recorded in $CDCl_3$ at room temperature unless noted otherwise. ^{11}B NMR spectroscopy (160 MHz) was performed at room temperature using a boron-free NMR tube, $CDCl_3$ as solvent, and $B(OH)_3$ in DMF as the external standard (referenced to 19.8 ppm).[20] All solvents (anhydrous or reagent-grade) were employed as received from commercial suppliers. Absorption and emission spectra were collected in toluene at room temperature. Silica (40 mm average particle size) was used for column chromatography. Si-diol (functionalized silica) TLC plates were purchased from SiliCycle. Commercial compounds were used as received unless noted otherwise. Compounds **2**,[18] **3**,[12] **5**,[12] **6**,[12] and **4-BBu$_2$**[16] were prepared as described in the literature.

8-Carbethoxy-10-(dibutylboryl)-2,3-dihydro-1,2,2-trimethyldipyrrin (1-BBu$_2$)

Following reported methods[12,16] with some modification, a solution of **8** (194 mg, 0.742 mmol) in DMF (7.1 mL) was treated with 6 M HCl (185 μL). After 15 min, NH_4OAc (1.2 g, 15 mmol) and triethylamine (2.1 mL, 15 mmol) were added. The resulting mixture was stirred overnight at room temperature and then quenched by the addition of saturated aqueous KH_2PO_4 solution. CH_2Cl_2 was added, and the organic layer was washed with water and brine, dried (Na_2SO_4) and concentrated. ^{1}H NMR analysis of the crude product indicated the presence of free base dihydrodipyrrins **1** and **1E** (estimated 4 : 1 ratio). TLC analysis [silica, hexanes/ethyl acetate (2 : 1)] showed one mobile component and material remaining at the origin, which were attributed to **1** and **1E**, respectively. Chromatographic separation proved difficult because of extensive streaking. Prior evidence indicates that the *E* and *Z* isomers of dihydrodipyrrins can interconvert under some reaction conditions.[34] Accordingly, the crude mixture was then dissolved in CH_2Cl_2 (6.0 mL) and treated with triethylamine (0.36 mL, 2.6 mmol) and Bu_2B–OTf (1.5 mL of 1 M solution in CH_2Cl_2, 1.5 mmol). The reaction mixture was stirred at room temperature for 1 h then quenched by the addition of saturated aqueous $NaHCO_3$ solution. The organic layer was washed twice more with saturated aqueous $NaHCO_3$ solution, dried (Na_2SO_4) and concentrated. Column chromatography [silica, hexanes/ethyl acetate (8 : 1 to 4 : 1)] afforded a yellow solid (149 mg, 52%): mp 118–120 °C; ^{11}B NMR δ 3.21; ^{1}H NMR ($CDCl_3$, 400 MHz) δ 7.40 (d, J = 1.5 Hz, 1H), 6.46 (s, 1H), 6.14 (s, 1H), 4.26 (q, J = 7.1 Hz, 2H), 2.67 (d, J = 1.8 Hz, 2H), 2.38 (s, 3H), 1.34 (t, J = 7.1 Hz, 3H), 1.27 (s, 6H), 1.20–1.07 (m, 4H), 0.92–0.57 (m, 15H); ^{13}C NMR ($CDCl_3$, 100 MHz) δ 186.2, 165.9, 137.1, 130.8, 129.2, 116.3, 111.2, 108.4, 59.3, 48.5, 40.1, 27.7, 26.1, 25.9, 14.7, 14.4, 14.3; ESI-MS obsd 385.3017, calcd 385.3021 [$(M + H)^+$, M = $C_{23}H_{37}BN_2O_2$]; λ_{abs} (toluene) 398 nm; λ_{em} (toluene) 506 nm.

7-Bromo-8-carbethoxy-10-(dibutylboryl)-2,3-dihydro-1,2,2-trimethyldipyrrin (2-BBu$_2$)

Following a reported method[16] with some modification, a solution of **2** (76 mg, 0.22 mmol) in CH_2Cl_2 (1.5 mL) was treated with triethylamine (0.11 mL, 0.79 mmol) and Bu_2B–OTf (0.45 mL of 1 M solution in CH_2Cl_2, 0.45 mmol). The reaction mixture was stirred at room temperature for 1 h and then quenched by the addition of saturated aqueous $NaHCO_3$ solution. The organic layer was washed twice more with saturated aqueous $NaHCO_3$ solution, dried (Na_2SO_4) and concentrated. Column chromatography [silica, hexanes/ethyl acetate (5 : 1)] afforded a yellow solid (88 mg, 85%): mp >117 °C (dec.); ^{11}B NMR δ 3.70; ^{1}H NMR ($CDCl_3$, 400 MHz) δ 7.39 (s, 1H), 6.30 (s, 1H), 4.29 (q, J = 7.1 Hz, 2H), 2.70 (d, J = 1.6 Hz, 2H), 2.38 (s, 3H), 1.36 (t, J = 7.1 Hz, 3H), 1.29 (s, 6H), 1.20–1.08 (m, 4H), 0.89–0.54 (m, 14H); ^{13}C NMR ($CDCl_3$, 100 MHz) δ 187.5, 164.4,

138.4, 130.9, 128.4, 114.5, 108.8, 95.7, 59.6, 48.7, 40.2, 27.6, 26.1, 25.9, 14.7, 14.6, 14.3; ESI-MS obsd 463.2131, calcd 463.2126 [(M + H)$^+$, M = $C_{23}H_{36}BBrN_2O_2$]; λ_{abs} (toluene) 398 nm; λ_{em} (toluene) 506 nm.

7-Bromo-8-carbethoxy-10-(difluoroboryl)-2,3-dihydro-1,2,2-trimethyldipyrrin (2-BF_2)

Following a reported method[2] with some modification, a solution of **2** (17 mg, 50 μmol) in anhydrous CH_2Cl_2 (1.0 mL) was treated with triethylamine (110 μL, 750 μmol) and $BF_3{\cdot}OEt_2$ (170 μL, 1.3 μmol). The reaction mixture was stirred at room temperature for 2 h and then loaded onto a silica column. Chromatography (silica, CH_2Cl_2) afforded a yellow solid (18 mg, 93%): mp >128 °C (dec.); ^{11}B NMR δ 0.95; ^{1}H NMR ($CDCl_3$, 400 MHz) δ 7.68 (s, 1H), 6.38 (s, 1H), 4.29 (q, J = 7.1 Hz, 2H), 2.78 (d, J = 2.0 Hz, 2H), 2.59 (s, 3H), 1.35 (t, J = 7.1 Hz, 3H), 1.35 (s, 6H); ^{13}C NMR ($CDCl_3$, 100 MHz) δ 195.7, 163.6, 137.5, 130.0, 128.8, 116.3, 107.8, 97.8, 59.8, 49.7, 40.1, 25.5, 14.6; ESI-MS obsd 387.0691, calcd 387.0686 [(M + H)$^+$, M = $C_{23}H_{36}BrN_2O_2$]; λ_{abs} (toluene) 400 nm; λ_{em} (toluene) 546 nm.

8-Carbethoxy-10-(dibutylboryl)-2,3-dihydro-5-(1-naphthyl)-1,2,2-trimethyldipyrrin (3-BBu_2)

Following a reported procedure,[16] a solution of **3** (50 mg, 0.13 mmol) and triethylamine (73 μL, 0.52 mmol) in CH_2Cl_2 (1.8 mL) was treated with Bu_2B–OTf (0.26 mL, 1 M in CH_2Cl_2, 0.26 mmol) under argon at room temperature. The reaction mixture was stirred for 3 h under argon. The reaction mixture was quenched with water and then extracted with CH_2Cl_2 (2 × 30 mL). The organic phase was dried (Na_2SO_4), concentrated, and chromatographed [silica, hexanes/ethyl acetate (4 : 1)] to afford a light yellow oil (48 mg, 71%): ^{11}B NMR δ 3.45; ^{1}H NMR δ 7.90 (d, J = 8.1 Hz, 2H), 7.77 (d, J = 8.2 Hz, 1H), 7.59–7.36 (m, 5H), 5.89 (d, J = 1.5 Hz, 1H), 4.20–4.10 (m, 2H), 2.45 (s, 3H), 2.26 (ABq, $\Delta\delta_{AB}$ = 0.12, J = 17.4 Hz, 2H), 1.37–1.08 (m, 15H), 0.99–0.71 (m, 12H); ^{13}C NMR δ 186.3, 165.8, 135.6, 133.9, 133.7, 132.0, 131.4, 131.0, 128.55, 128.46, 127.2, 126.6, 126.1, 125.6, 125.3, 123.8, 116.3, 109.3, 59.3, 48.3, 39.5, 28.3, 27.8, 26.2, 26.09, 26.08, 25.9, 14.7, 14.6, 14.5, 14.4; ESI-MS obsd 511.3494, calcd 511.3490 [(M + H)$^+$, M = $C_{33}H_{43}BN_2O_2$]; λ_{abs} (toluene) 411 nm; λ_{em} (toluene) 503 nm; λ_{abs} (CH_2Cl_2) 388 nm.

8-Carbethoxy-10-(difluoroboryl)-2,3-dihydro-5-(1-naphthyl)-1,2,2-trimethyldipyrrin (3-BF_2)

Following a reported method[2] with some modification, a solution of **3** (0.180 g, 0.466 mmol) and triethylamine (0.33 mL, 2.3 mmol) in CH_2Cl_2 (6.0 mL) was treated with $BF_3{\cdot}OEt_2$ (0.58 mL, 4.66 mmol) under argon at room temperature. The reaction mixture was stirred overnight under argon. The reaction mixture was quenched by addition of saturated aqueous $NaHCO_3$ (20 mL) and then extracted with CH_2Cl_2 (2 × 50 mL). The organic phase was dried (Na_2SO_4), concentrated, and chromatographed [silica, hexanes/ethyl acetate (2 : 1)] to afford a light yellow solid (0.180 g, 86%): mp 222–224 °C; ^{11}B NMR δ 1.28 (a peak between 0 and −1 ppm was unassigned and may stem from slight decomposition); ^{1}H NMR δ 7.91 (d, J = 8.1 Hz, 2H), 7.79–7.73 (m, 2H), 7.57–7.38 (m, 4H), 6.00 (s, 1H), 4.17 (q, J = 7.1 Hz, 2H), 2.66 (s, 3H), 2.38 (ABq, $\Delta\delta_{AB}$ = 0.08, J = 17.4 Hz, 2H), 1.29–1.21 (m, 9H); ^{13}C NMR δ 194.4, 165.1, 134.7, 133.9, 132.2, 131.1, 129.9, 128.9, 128.7, 127.2, 126.8, 126.3, 125.6, 125.1, 122.8, 118.4, 111.0, 59.6, 49.3, 39.6, 25.4, 14.6; ESI-MS obsd 435.2059, calcd 435.2050 [(M + H)$^+$, M = $C_{25}H_{25}BF_2N_2O_2$]; λ_{abs} (toluene) 401 nm; λ_{em} (toluene) 550 nm; λ_{abs} 388 nm (CH_2Cl_2).

4-Ethoxycarbonyl-(*E*)-2-[(4,4-dimethyl-5-oxodihydrofuran-2(3*H*)-ylidene)methyl]pyrrole (7)[12]

Following a reported procedure[12] with slight modification, a solution of pyrrole **5** (11.8 g, 44.5 mmol), pentynoic acid **6** (11.23 g, 89.01 mmol), and $BnEt_3NCl$ (11.15 g, 48.95 mmol) in anhydrous MeCN (191 mL) and triethylamine (105 mL) was deaerated by two freeze–pump–thaw cycles. $Pd(PPh_3)_4$ (1.54 g, 1.34 mmol) was then added. The resulting mixture was heated to 60 °C for 2 h and then allowed to cool to room temperature. The reaction mixture was diluted with CH_2Cl_2 (200 mL) and washed with 1 M HCl (710 mL) and brine (200 mL). The organic layer was dried (Na_2SO_4) and concentrated under reduced pressure. Column chromatography [silica, CH_2Cl_2/acetone (30 : 1 to 8 : 1)] afforded a white solid (9.43 g, 80%): mp 132–134 °C; ^{1}H NMR (400 MHz, $CDCl_3$) δ 1.35 (s, 6H), 1.35 (t, J = 7.1 Hz, 3H), 4.29 (q, J = 7.1 Hz, 2H), 6.15 (dd, J = 2.0, 1.6 Hz, 1H), 6.39 (s, 1H), 7.39 (dd, J = 3.0, 1.6 Hz, 1H), 9.00 (br s, 1H); ^{13}C NMR (100 MHz, $CDCl_3$) δ 14.6, 25.4, 40.1, 40.6, 60.1, 97.6, 107.0, 117.8, 123.5, 127.5, 148.3, 165.2, 180.1; ESI-MS obsd 264.1231, calcd 264.1230 [(M + H)$^+$, M = $C_{14}H_{17}NO_4$].

4-Carbethoxy-(*E*)-2-[(4,4-dimethyl-5-methylenedihydrofuran-2(3*H*)-ylidene)methyl]pyrrole (8)

Following a reported method[12] with some modification, a solution of $TiCp_2Cl_2$ (1.77 g, 7.11 mmol) in toluene (19.0 mL) was treated dropwise with MeLi (9.7 mL of 1.6 M solution in Et_2O, 16 mmol) over 5 min at 0 °C under an argon atmosphere. After 1 h at 0 °C, the reaction was quenched by the addition of 6% aqueous NH_4Cl solution. The organic layer was washed with water and brine, dried (Na_2SO_4) and filtered. The filtrate was treated with lactone–pyrrole **7** (394 mg, 1.50 mmol) and additional $TiCp_2Cl_2$ (22 mg, 88 μmol). The mixture was heated to 80 °C in the dark for 4 h and then allowed to cool to room temperature, whereupon $NaHCO_3$ (75 mg), MeOH (1.8 mL) and H_2O (1.8 μL, 0.1% v/v relative to MeOH) were added. The mixture was then stirred overnight at 40 °C. The reaction mixture was filtered through Celite. The filtrate was concentrated and chromatographed (silica, CH_2Cl_2 with 0–5% ethyl acetate) to afford a yellow-brown solid (271 mg, 69%): mp 99–100 °C; ^{1}H NMR ($CDCl_3$, 300 MHz) δ 8.24 (b, 1H), 7.33 (dd, J = 3.0, 1.5 Hz, 1H), 6.35–6.29 (m, 1H), 5.83 (dt, J = 2.0, 1.0 Hz, 1H), 4.39 (d, J = 2.4 Hz, 1H), 4.28 (q, J = 7.1 Hz, 2H), 4.01 (d, J = 2.4 Hz, 1H), 2.71 (d, J = 1.9 Hz, 2H), 1.34 (t, J = 7.1 Hz, 3H), 1.26 (s, 6H); ^{13}C NMR ($CDCl_3$, 75 MHz) δ 169.6, 165.1, 155.0, 129.6, 122.4, 117.8, 105.7, 92.2, 80.9, 59.9, 42.7, 40.2, 28.1, 14.7.

Photophysical measurements

Photophysical studies in toluene (and for one compound in acetonitrile and dimethylsulfoxide) were carried out on dilute (μM)

argon-purged solutions. Fluorescence quantum yields were determined for deoxygenated samples relative to the standards pyranine (Φ_f = 1.0 in 0.10 M NaOH[23]) and 5-mesityldipyrrinatoboron difluoride (BDPY1) (Φ_f = 0.93 in toluene[24]). S_1 lifetimes were determined by time correlated single photon counting (TCSPC) fluorescence spectroscopy and by transient absorption (TA) spectroscopy, both employing ~100 fs excitation flashes from an ultrafast laser system (Spectra Physics). TCSPC studies utilized a simple-Tau 130 system (Becker & Hickl) with an instrument response function of <200 ps using ~100 fs visible-region excitation pulses (at 8 MHz) attenuated to avoid exciton annihilation. Acquisition of TA difference spectra (400–900 nm) from ~100 fs to ~7.5 ns utilized a spectrometer that employed ~100 fs white-light probe pulses (Ultrafast Systems, Helios) and on the time scale from ~100 ps to ~0.5 ms using a white-light pulsed laser (~1 ns rise time) in 100-ps time bins with pump–probe delay to 0.5 ms (Ultrafast Systems, EOS). TA studies also afforded the yield of $S_1 \rightarrow T_1$ intersystem crossing by comparing the extent of bleaching of the ground-state absorption bands due to T_1 at the asymptote of the S_1 decay *versus* the extent due to S_1 immediately after excitation. TA data sets were analyzed at individual wavelengths and globally using Surface Explorer (Ultrafast Systems), CarpetView (Light Conversions) and OriginPro (Origin Labs). Time profiles were fit to the convolution of the instrument response with a series of exponentials plus a constant.

Density functional theory calculations

DFT calculations were performed with Gaussian 09 version D.01.[35] Calculations used the polarization continuum model in toluene, acetonitrile and dimethylsulfoxide. Molecular geometries were fully optimized using the hybrid B3LYP functional and the basis set 6-31G*. These calculations used Gaussian defaults with the exception of keyword Int = (Grid = Ultrafine, Acc2E = 14). TDDFT calculations used the long-range corrected ωB97XD functional and the basis set 6-31++G**. These calculations used Gaussian defaults with the exception of keywords TD (nStates = 16), Int = (Grid = Ultrafine, Acc2E = 14), and Pop = Full.

Conflicts of interest

The authors declare no competing financial conflicts of interest.

Acknowledgements

This work was funded by the Division of Chemical Sciences, Geosciences, and Biosciences, Office of Basic Energy Sciences of the U.S. Department of the Energy (FG02-05ER15661). Mass spectrometry data were obtained in the Molecular Education, Technology, and Research Innovation Center (METRIC) at NC State University. The time-resolved optical data were acquired in the Ultrafast Laser Facility of the Photosynthetic Antenna Research Center, an Energy Frontier Research Center supported by the U.S. Department of Energy, Office of Science, Office of Basic Energy Sciences, under Award No. DE-SC0001035.

References

1 A. Treibs and F.-H. Kreuzer, *Liebigs Ann. Chem.*, 1968, **718**, 208–223.
2 R. W. Wagner and J. S. Lindsey, *Pure Appl. Chem.*, 1996, **68**, 1373–1380. Corrigendum: R. W. Wagner and J. S. Lindsey, *Pure Appl. Chem.*, 1998, **70**(8), p.i.
3 A. Loudet and K. Burgess, *Chem. Rev.*, 2007, **107**, 4891–4932.
4 R. Ziessel, G. Ulrich and A. Harriman, *New J. Chem.*, 2007, **31**, 496–501.
5 A. C. Benniston and G. Copley, *Phys. Chem. Chem. Phys.*, 2009, **11**, 4124–4131.
6 N. Boens, V. Leen and W. Dehaen, *Chem. Soc. Rev.*, 2012, **41**, 1130–1172.
7 S. G. Awuah and Y. You, *RSC Adv.*, 2012, **2**, 11169–11183.
8 Y. Ni and J. Wu, *Org. Biomol. Chem.*, 2014, **12**, 3774–3791.
9 T. Kowada, H. Maeda and K. Kikuchi, *Chem. Soc. Rev.*, 2015, **44**, 4953–4972.
10 J. Bañuelos, *Chem. Rec.*, 2016, **16**, 335–348.
11 Y. V. Zatsikha and Y. P. Kovtun, in *Handbook of Porphyrin Science*, ed. K. M. Kadish, K. M. Smith and R. Guilard, World Scientific Publishing Co. Pte. Ltd, Singapore, 2016, ch. 182, vol. 36, pp. 151–257.
12 Y. Liu and J. S. Lindsey, *J. Org. Chem.*, 2016, **81**, 11882–11897.
13 S. Zhang, M. N. Reddy, O. Mass, H.-J. Kim, G. Hu and J. S. Lindsey, *New J. Chem.*, 2017, **19**, 11170–11189.
14 K. Muthukumaran, M. Ptaszek, B. Noll, W. R. Scheidt and J. S. Lindsey, *J. Org. Chem.*, 2004, **69**, 5354–5364.
15 S. H. H. Zaidi, K. Muthukumaran, S.-I. Tamaru and J. S. Lindsey, *J. Org. Chem.*, 2004, **69**, 8356–8365.
16 M. Liu, M. Ptaszek, O. Mass, D. J. Minkler, R. D. Sommer, J. Bhaumik and J. S. Lindsey, *New J. Chem.*, 2014, **38**, 1717–1730.
17 X. Liu, J. M. Cole, P. G. Waddell, T.-C. Lin, J. Radia and A. Zeidler, *J. Phys. Chem. A*, 2012, **116**, 727–737.
18 H. Fujita, H. Jing, M. Krayer, S. Allu, G. Veeraraghavaiah, Z. Wu, J. Jiang, J. R. Diers, N. C. M. Magdaong, A. K. Mandal, A. Roy, D. M. Niedzwiedzki, C. Kirmaier, D. F. Bocian, D. Holten and J. S. Lindsey, *New J. Chem.*, 2019, DOI: 10.1039/c9nj01113g.
19 I. Ghosh and P. A. Jacobi, *J. Org. Chem.*, 2002, **67**, 9304–9309.
20 M. J. S. Dewar and R. Jones, *J. Am. Chem. Soc.*, 1967, **89**, 2408–2410.
21 B. Wrackmeyer and B. Schwarze, *J. Organomet. Chem.*, 1997, **534**, 207–211.
22 B. Wrackmeyer, *Annu. Rep. NMR Spectrosc.*, 1988, **20**, 61–203.
23 T. H. Tran-Thi, C. Prayer, P. Millié, P. Uznanski and J. T. Hynes, *J. Phys. Chem. A*, 2002, **106**, 2244–2255.
24 H. L. Kee, C. Kirmaier, L. Yu, P. Thamyongkit, W. J. Youngblood, M. E. Calder, L. Ramos, B. C. Noll, D. F. Bocian, W. R. Scheidt, R. R. Birge, J. S. Lindsey and D. Holten, *J. Phys. Chem. B*, 2005, **109**, 20433–20443.
25 J. B. Birks, *Photophysics of Aromatic Molecules*, Wiley-Interscience, London, 1970.
26 F. Li, S. I. Yang, Y. Ciringh, J. Seth, C. H. Martin III, D. L. Singh, D. Kim, R. R. Birge, D. F. Bocian, D. Holten and J. S. Lindsey, *J. Am. Chem. Soc.*, 1998, **120**, 10001–10017.

27 S. Nad and H. Pal, *J. Phys. Chem. A*, 2001, **105**, 1097–1106.
28 K. Das, B. Jain and H. S. Patel, *J. Phys. Chem. A*, 2006, **110**, 1698–1704.
29 J. Bañuelos, V. Martín, C. F. A. Gómez-Durán, I. J. A. Córdoba, E. Peña-Cabrera, I. García-Moreno, Á. Costela, M. E. Pérez-Ojeda, T. Arbeloa and Í. L. Arbeloa, *Chem. – Eur. J.*, 2011, **17**, 7261–7270.
30 R. I. Roacho, A. Metta-Magaña, M. M. Portillo, E. Peña-Cabrera and K. H. Pannell, *J. Org. Chem.*, 2013, **78**, 4245–4250.
31 M. Taniguchi and J. S. Lindsey, *Photochem. Photobiol.*, 2018, **94**, 290–327.
32 Q. Qi, M. Taniguchi and J. S. Lindsey, *J. Chem. Inf. Model.*, 2019, **59**, 652–667.
33 M. V. Sednev, V. N. Belov and S. W. Hell, *Methods Appl. Fluoresc.*, 2015, **3**, 042004.
34 Y. Liu, S. Allu, M. N. Reddy, D. Hood, J. R. Diers, D. F. Bocian, D. Holten and J. S. Lindsey, *New J. Chem.*, 2017, **41**, 4360–4376.
35 M. J. Frisch, G. W. Trucks, H. B. Schlegel, G. E. Scuseria, M. A. Robb, J. R. Cheeseman, G. Scalmani, V. Barone, B. Mennucci, G. A. Petersson, H. Nakatsuji, M. Caricato, X. Li, H. P. Hratchian, A. F. Izmaylov, J. Bloino, G. Zheng, J. L. Sonnenberg, M. Hada, M. Ehara, K. Toyota, R. Fukuda, J. Hasegawa, M. Ishida, T. Nakajima, Y. Honda, O. Kitao, H. Nakai, T. Vreven, J. A. Montgomery Jr., J. E. Peralta, F. Ogliaro, M. Bearpark, J. J. Heyd, E. Brothers, K. N. Kudin, V. N. Staroverov, R. Kobayashi, J. Normand, K. Raghavachari, A. Rendell, J. C. Burant, S. S. Iyengar, J. Tomasi, M. Cossi, N. Rega, J. M. Millam, M. Klene, J. E. Knox, J. B. Cross, V. Bakken, C. Adamo, J. Jaramillo, R. Gomperts, R. E. Stratmann, O. Yazyev, A. J. Austin, R. Cammi, C. Pomelli, J. W. Ochterski, R. L. Martin, K. Morokuma, V. G. Zakrzewski, G. A. Voth, P. Salvador, J. J. Dannenberg, S. Dapprich, A. D. Daniels, Ö. Farkas, J. B. Foresman, J. V. Ortiz, J. Cioslowski and D. J. Fox, *Gaussian 09, version D.01*, Gaussian, Inc., Wallingford, CT, 2009.

